

Improving the Oxygen Barrier of Polyamide Food Packaging by Using Nanoclay

Tõnis PAARA^{1*}, Sven LANGE¹, Kristjan SAAL¹, Rünno LÕHMUS¹, Andres KRUMME², Hugo MÄNDAR¹

¹ Institute of Physics, University of Tartu, W. Ostwaldi 1, 50411 Tartu, Estonia

² Department of Polymeric Materials, Tallinn University of Technology, Ehitajate tee 5, Tallinn, Estonia

crossref <http://dx.doi.org/10.5755/j02.ms.28868>

Received 12 April 2021; accepted 23 June 2021

The effect of nanoclay additive on polyamide film oxygen permeability is investigated from the perspective of possible use as a laminate component for low-cost food packaging material. Montmorillonite nanoclay was melt-mixed in an industrial grade polyamide by twin-screw extrusion and the mixture was hot-pressed to a ~50 µm thick film. The film with 10 wt.% of nanoclay loading showed a 17 % decrease in the oxygen transmission rate (OTR), as compared to the pristine polyamide film (72 and 87 cm³/m²·24 h, respectively). Despite the relatively high loading of the filler the obtained OTR exceeds that of the food packaging preferred upper limit of 10 cm³/m²·24 h. XRD measurements confirmed the near-complete exfoliation of the nanoclay platelets. The platelets were found to be at an average angle of 9.5 degrees relative to the film's surface plane. To comply with the requirements for food packaging, this angle needs to be decreased down to 0.4 degrees. To achieve this, different film-making methods enabling better control over the filler particles' orientation need to be explored. Nanoclay addition increased the films' yield strength (23 % for 10 wt.% film) and stiffness, while not affecting the films' optical appearance.

Keywords: nanoclay, polyamide, composite, oxygen transmission rate, nano-additives, food packaging, nanocomposite, gas barrier.

1. INTRODUCTION

Modern storage and transportation of food products require packaging that is lightweight, durable, and able to sustain the enclosed gas composition for a prolonged period of time. Upon storing in an artificial inert atmosphere, the product is sealed against moisture and oxygen, of which the latter poses a superior challenge for a barrier because of its vastly greater permeability in most packaging materials. Oxygen is the known cause of unwanted microbiological activity, colour change and spoilage of food. To protect the product from oxygen, modified atmosphere packaging (MAP) is widely used by food processing industries. In the case of MAP, the package is filled with N₂ and/or CO₂, with a reduced oxygen concentration of 0.5–2 %. The package barrier material must ensure a low enough diffusion coefficient for oxygen to sustain the modified atmosphere throughout the supply chain. Industrially, any OTR value below 10 cm³/m²·24 h is considered sufficiently low for most medium-term storage [1].

Thermopolymers conventionally used in food packaging do not meet that requirement. The cheapest but relatively durable and therefore most common packaging polymers make very poor oxygen barriers: i.e. 25-micron low density polyethylene (LDPE) film has an OTR of 8586 cm³/m²·24 h, while this of 25 µm polypropylene film is 2526 cm³/m²·24 h [2]. Polymers with better oxygen barrier tend to be more expensive and are therefore used as one layer of a laminate. Most notably, 25 µm polyethylene terephthalate (PET) film has an OTR of ~35 cm³/m²·24 h and 25 µm polyamide (PA) ~25 cm³/m²·24 h. To improve

the barrier properties, active or passive additives can be applied to the polymer. In the case of active additives, the so-called oxygen scavengers chemically target the impregnating oxygen. The scavengers can vary greatly either by type (organic, inorganic) or by action mechanism (removing oxygen directly or slowing down the radical oxidation reactions). The active barriers have shown great efficiency and are therefore well-suited for the products where even the slightest contact with oxygen is undesirable during the shelf-life period. Passive barriers often do not comply with these specifications. Despite this they can have some advantages over the active barriers. First, the majority of active barriers affect the transparency and coloration of the polymer because most scavengers are opaque or coloured, and the colour can change during oxidation of the scavenger (e.g. iron to iron oxide). Also, active barriers tend to be more expensive, and their recycling is not favoured because of the accumulation of the oxidized scavenger in the polymer. The most common passive barriers, on the other hand, are cheap and transparent (silica, clay) and the packages can be recycled. Given the huge circulation of foodstuff products, as compared to other oxygen sensitive products such as flexible LCD, OLED and solar cells, the combination of low cost and unaltered appearance of the package polymer makes the passive barriers attractive for the foodstuff packaging application. As for the foodstuff packaging materials, PE, PP and PET are the most widely used because of their low cost (PE and PP for food, PET for beverages). Both PE and PP have very high OTR, which cannot be lowered to the required minimum value of 10 cm³/m²·24 h just by the addition of additives. To achieve

* Corresponding author. Tel.: +372 53761232
E-mail address: tpaara@gmail.com

this, laminates with polymers of higher barrier properties are used. However, meeting the required OTR still takes a rather thick layer of the latter, which adds to the total polymer consumption in the package. In order to address this problem, the OTR reducing additives can be applied in the laminated high barrier polymer film, rendering it efficient at a considerably lower thickness. In most polymers, loosely spaced, but oriented nanoclay can form a continuous tortuous path for diffusing gas molecules, allowing to decrease of the OTR by 2–3 times already at moderate doping levels (~10 wt.%) [3, 4], but decrease by even an order of magnitude has been reported [5]. In the present work, we show that it is possible to decrease the OTR of a high barrier laminate film, namely PA, further via the inclusion of nano-scale clay platelets into the polymer. We use functionalized montmorillonite nanoclay, which consists of small clay platelets that act as a physical barrier against the impregnating oxygen. Nanoclay and PA mixtures have been studied before for such a purpose, but to our knowledge not beyond the 3 wt.% loading [6]. We hereby will test the loading of up to 10 wt.% and use a commercial PA masterbatch to assess its potential applicability as a low-cost food storage packaging material.

2. EXPERIMENTAL DETAILS

In order to prepare a homogenous mixture of dispersed and exfoliated nanoclay in PA matrix, the nanoclay was first mixed with ground PA granules and then melt extruded with a lab scale twin screw extruder.

The nanoclay used in this experiment was Nanomer I.28E (Nanocor Inc.). This specific grade was chosen due to its cetyl trimethyl ammonium surface functionalization, which helps further dispersion and exfoliation of the clay platelets within the matrix according to Nanocor Inc. The polymer used in this research was an industrial-grade PA (polyamide)6/6.6, which was received in granulated form (granule diameter 2–3 mm) from an industrial partner Estiko Plastar AS. Twin-screw extrusion was chosen as the method of mixing to replicate the real industrial processing of polymers as much as possible. This was done in hopes of developing a method that could also be sufficient for industrially viable production. The PA granules were ground into thin shavings about 1 mm in diameter by using a rotary grater, in order to speed up the extrusion process – it reduces the time needed for melting the polymer and increases the homogeneity of the nanoclay-PA mixture.

The samples were prepared by two different recipes: 2 % and 10 % of nanoclay by weight were added to the PA matrix and mixed thoroughly for 15 minutes in a twin-screw lab extruder with a backflow channel. The mixing time was kept relatively short to avoid polymer degradation and damage to the nanoclay surface modification. The backflow channel was used for creating high-shear turn points for the moving molten mass, which helps to mix, exfoliate, and separate the nanoclay platelets.

In order to produce large-scale thin film samples ($\varnothing 80$ mm) required for OTR measurements, the composite was once again granulated, then melted and flattened by using a heated hydraulic platen press. The teflon lining was used in the custom-made mould to avoid damaging the sample upon removal.

The prepared samples were then inspected under an optical microscope, scanning electron microscope (FEI SEM NanoSem 450) and transmission electron microscope (FEI TEM Tecnai 10). The OTR measurements were carried out by using the ISO standardized (ISO 15105-1) Labthink PERME@VAC-VBS Gas Permeability Tester. The tensile properties were measured on a Zwick/Roell 500N tensile tester according to ISO 527-3 standard.

X-ray diffraction analysis (XRD) of nanoclay was performed on a diffractometer by SmartLab™ (Rigaku, Japan) using Cu rotating anode operated at 45 kV and 180 mA, with a coordinate sensitive 1D detector D/teX Ultra (for WAXS range in Bragg-Brentano optical setup) or 0D scintillation detector (for WAXS using parallel beam optics, and for transmission SAXS range implementing SAXS optics). The diffraction pattern was recorded between diffraction angles of 8 and 80° or 2 and 10° with a step size of 0.01° or 0.04 (2 θ) and a scan speed of 5 deg/min or 1.5 deg/min by using Bragg-Brentano or parallel beam optics, correspondingly. The SAXS patterns were scanned between 0.1 and 10° with a step size of 0.02° (2 θ) and a scan speed of 1 deg/min. The nanoclay powder, prepared for the reflection analysis, was slightly pressed into a 0.5 × 20 × 20 mm³ quartz cuvette. The composite sample consisted of ten layers of polymer film (thickness ~1 mm) and was measured both in the transmission and reflection modes.

3. RESULTS AND DISCUSSION

Nanoclay was largely agglomerated prior to mixing with polyamide. SEM imaging revealed agglomerates of nanoclay platelets of up to several dozens of micrometers in diameter (Fig. 1). The single platelets were a few tens of nanometers thick and up to a few micrometers wide (Fig. 2).

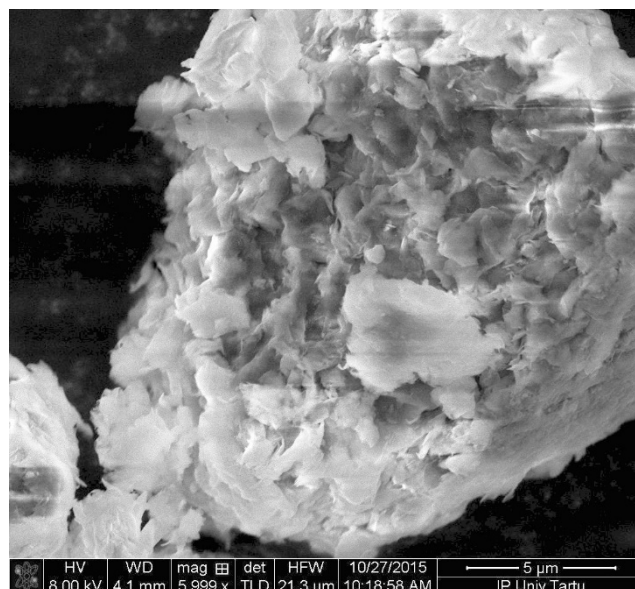


Fig. 1. SEM image of nanoclay agglomerate before to mixing with PA

The prepared film samples of the PA–nanoclay mixture were ~50 μm thick, optically transparent without any visible agglomerates and had a slight brown hue – not enough to compromise the commercial appearance.

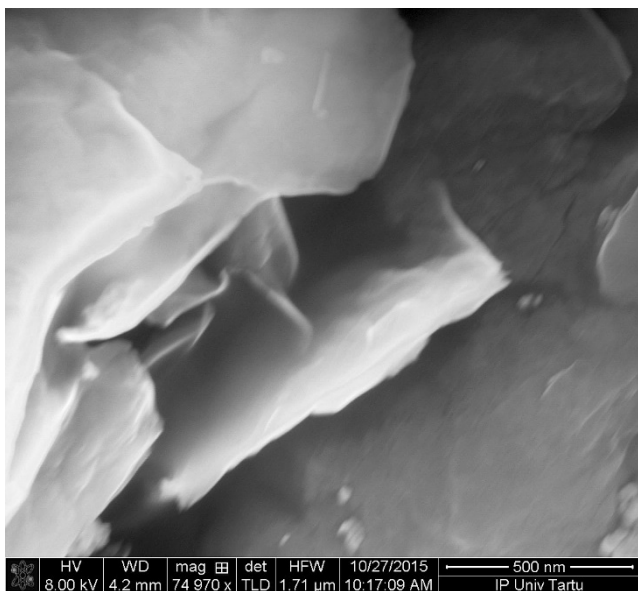


Fig. 2. SEM close-up of a nanoclay agglomerate before to mixing with PA

The nanoclay-doped samples were also somewhat stiffer than the reference samples, which caused them to crack more easily upon removal from the mold. This is in concurrence with previous studies which have shown an increase in the elastic modulus of nanoclay-polymer composites [7]. The increased elastic modulus could be beneficial for sustaining the structural integrity of the packaging material with the laminated layer being thinner than the untreated analogue.

SEM imaging revealed some agglomerates and non-exfoliated nanoclay clusters on the surface of the polymer surrounded by probably single nanoclay platelets (see Fig. 3). This demonstrates that the exfoliation process had taken place, but not exhaustively, since some of the nanoclay material remained in agglomerated form, reducing the potential barrier effect of the additive. The electron beam of the SEM is unable to penetrate the polymer surface and therefore it is impossible to observe the distribution of the features inside the film.



Fig. 3. Nanoclay single particles and unexfoliated agglomerates in the film skin layer

In order to get a better view of the level of dispersion and exfoliation of nanoclay particles, a microtome was used

to cut a thin (140 nm) slice from the mixed and extruded PA-nanoclay filament. The slice was investigated under TEM, which revealed the inner structure of the sample. The size of the agglomerates varied: 1–2 μm in length on average, with thicknesses in the range of 10–50 nm (Fig. 4). It is worth mentioning that since single nanoclay platelets can be as thin as 1 nm, they would be very difficult to detect when perpendicular to the viewing angle, thus more likely the observed thickness indicates that the sheets were at different angles with respect to the direction of observation. This gives an indication that the exfoliation process had certainly taken place to some extent. We cannot rule out that some of the observed features were in fact multilayer agglomerates and therefore cannot confirm that the nanoclay-polymer mixing by twin-screw extrusion is sufficient to separate all the agglomerates.

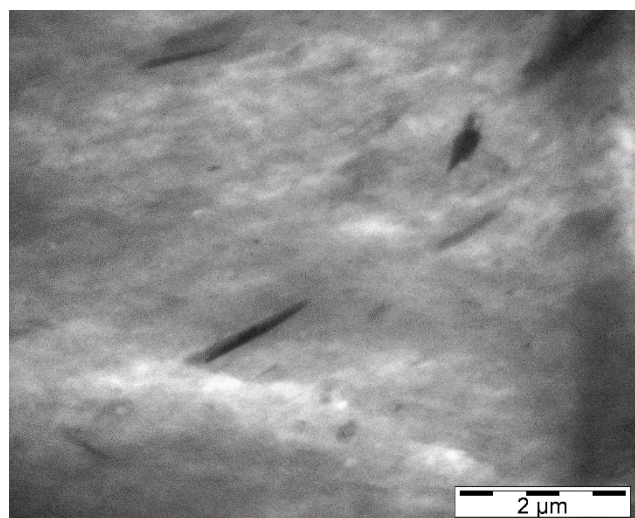


Fig. 4. TEM image of nanoclay platelets in polyamide (PA) film cross-section

Further confirmation of the exfoliation is evident from the XRD analysis. Fig. 5 shows the XRD pattern of the pure nanoclay sample. The first strong reflection at $2\theta = 4.2^\circ$ (d-spacing = 2.1 nm) can be assigned to the (001) basal plane of nanoclay. The value of d-spacing is close to those reported in other studies that have used Nanomer I.28E as a reinforcing material, e.g. 1.8 nm [8], 2.258 nm [9], 2.4 nm [10], 2.49 nm [11], 2.535 nm [12]. Most of the other reflections of this sample can be indexed based on structure data of triclinic montmorillonite (MMT) from the ICSD database (collection code 51636) and replacing cell parameter $c = 1.56$ nm to $c = 2.1$ nm.

Fig. 6 depicts both SAXS (measured in transmission) and WAXS (measured in reflection) patterns for neat PA film, the nanoclay and the PA + 10 wt.% nanoclay composite. The SAXS patterns of neat PA film versus nanoclay+PA composite were almost identical - both patterns did not show any clear scattering reflections in the range of $2 - 10^\circ$ (2θ). Only a slight change in the decay of the intensity at $2\theta = 0.6 - 1.2^\circ$ can be observed on both patterns. Pattern decomposition and fitting at this range showed that a broad (FWHM = 1.2°) reflection at $2\theta = 0.96^\circ$ (d-spacing = 9.1 nm) was responsible for this hump in the decay. Since this reflection with the same shape and intensity was observed also on the XRD pattern of neat

PA we can assign its origin unambiguously to the polymer structure of the PA.

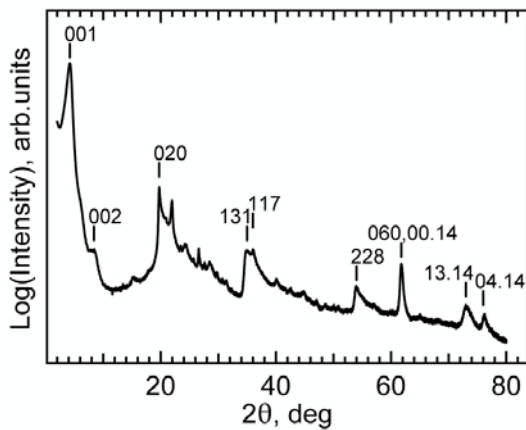


Fig. 5. WAXS pattern of pure nanoclay. The strongest reflections are labeled by Miller indices of corresponding crystallographic planes. The first part of the pattern from 2° to 8° was measured using parallel beam optics and the rest by Bragg-Brentano optics

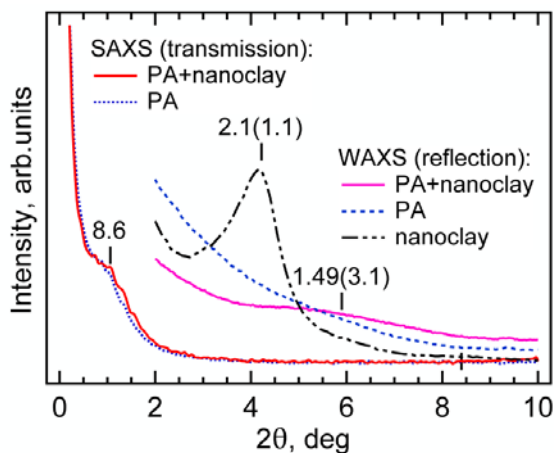


Fig. 6. SAXS and WAXS patterns for neat polyamide film (PA), the nanoclay and the composite PA + 10 wt.% nanoclay. The WAXS patterns are scaled down to 1:50 to match into the low intensity scale of the SAXS patterns. The first part of the WAXS pattern of nanoclay is presented for showing the shape and locations of the 001 reflection in more detail. The label at the position of a reflection shows the corresponding lattice spacing in nanometers and the values in parentheses are full width at half maximum (FWHM, $^\circ$) of the reflections

This assumption is consistent also with the results of previous SAXS analysis [13] showing that a broad and weak reflection at scattering vector modulus of approximately 0.5 1/nm (corresponding to $2\theta = 1.2^\circ$ for $\text{CuK}\alpha$ radiation) originates from mesostructure of PA (nylon-6) described by lamellar crystallites with a periodic spacing of 9.95 nm . Hence, it is reasonable to believe that the preparation process of the nanocomposite had not remarkably destroyed the lamellar structure of the PA matrix.

Appearance or disappearance of the basal reflection of nanoclay in the composite or its shift towards higher or lower diffraction angles compared to its position on the pattern of nanoclay (at $2\theta = 4.2^\circ$ in this work) enables to identify the type of polymer-clay composite and the rate of intercalation of the nanoclay in the polymer matrix [14, 15].

The absence of this reflection on the SAXS pattern of PA-nanoclay composite (Fig. 6, two leftmost curves) could point to completely exfoliated or delaminated nanoclay in PA. The other explanation for the missing basal reflection in the range of $2\theta = 2 - 10^\circ$ could be connected with the presence of preferential orientation of clay crystallites in the composite. By taking into account the high aspect ratio of nanoclay platelet and the fabrication process of PA-composite film by using hydraulic platen press, we can assume that the distribution function of angles between the normals of the (001) planes of clay crystallites and the film surface is narrow. The basal reflection from crystallites can for this type of preferential orientation be observed only in reflection mode of X-ray diffraction.

Fig. 6 depicts also the scattering curves measured in reflection mode (the three rightmost curves). The pattern from PA-nanoclay composite film exhibits a broad and weak peak located at $2\theta = 5.9^\circ$. This peak can unequivocally be identified as the basal 001 reflection from nanoclay in the composite because the pattern of neat PA did not show any peaks in this scattering range. The disappearance of this peak by transmission XRD and appearance by reflection XRD analysis confirms the assumption about the preferential orientation of clay crystallites in the PA-nanoclay composite. Abdelwaha et al. [16] observed a similar preferred orientation effect for polyamide-Nanomer I.30T composite produced by melt extrusion and injection molding, and explained the different behavior of basal reflection measured in reflection and transmission modes of XRD pattern by the anisotropic effect of the injection molding forcing the nanoclay platelets to be oriented preferentially parallel to the plane of the samples.

The d_{001} -spacing for clay crystallites in composite was approximately 1.4 times smaller compared to the pure nanoclay spacing of 2.1 nm . The results of previous researches have demonstrated that when using the organically treated montmorillonite (Nanomer I.28E) the sign of the change of basal d_{001} -spacing of nanoclay depends on the processing method and the material of the matrix. Yasmin et al. [10] have shown that intercalation of nanoclay in epoxy+nanoclay composite is accompanied by the increase of the d_{001} -spacing. This process in the polyester/glass fiber/nanoclay composites resulted in the decrease of d -spacing from 1.94 nm to 1.28 nm for samples with 6 wt.% of nanoclay [11]. The same result was observed also when using poly(ethylene oxide) (PEO) and nanoclay composite prepared by aqueous solution casting and direct melt press compounding techniques – d_{001} -spacing decreased from 2.26 nm in the case of pure nanoclay to 1.51 nm in the PEO + 20 wt.% nanoclay composite [9]. The other types of nanoclays in the polyamide-clay composites have shown also a decrease of the d_{001} -spacing that were explained by re-arrangement of the organic modifier present in the nanoclay caused by chemical interaction or the effects of shear during the extrusion process [17]. The latter process is presumably the most relevant for explaining the decrease of d_{001} -spacing in PA-nanoclay composite in this work.

Approximately a triple increase of the broadening of this reflection from 1.1° to 3.1° , that corresponds to decrease of the effective X-ray crystallite size from 6.4 nm to 2.6 nm , or decrease of the average number of clay layers in [001] direction of the crystallites from 3 to 1.7, was observed for

the nanoclay in the composite. This result can be explained by the appearance of partially exfoliated crystallites of nanoclay in the composite, but might also indicate an unevenly delaminated or polymer intercalation and gradients in d-spacings of the clay crystallites [16]. The low intensity of this reflection, related to the low concentration of partially exfoliated clay crystallites in the composite, allowed us to infer that the concentration of intercalated nanoclay crystallites is small and most of the silicate layers of crystallites in the nanocomposite were exfoliated or delaminated. This result is consistent with SEM and TEM analysis results that also observed only a minor amount of agglomerated or/and intercalated nanoclay crystallites in the composite film.

To evaluate the barrier effect of the nanoclay additive, the OTR of the prepared samples were compared to the pristine PA films. The samples with different nanoclay loading were measured at 23 °C and 30 % of relative humidity to mimic typical storage conditions (Table 1).

Table 1. Measured OTR for the prepared samples

% of nanoclay by weight	Oxygen transmission rate (cm ³ /m ² /24 h)
0 %	87(4)
2 %	82(4)
10 %	72(4)

As nanoclay concentration increases the OTR is expected to decrease. The reduction in OTR value is in turn influenced by the aspect ratio of the filler particles and has been shown to follow a law, introduced by Nielsen already in 1967 [18]:

$$\frac{P_f}{P_u} = \frac{\Phi_P}{1 + (L/2W) \Phi_F} \quad (1)$$

where P_f and P_u are transmission rates for filled and unfilled polymer, respectively; Φ_P and Φ_F volume ratios of polymer and filler, and L/W aspect ratio of the filler particles; L is short for length and W for width. The relation indicates that it should be possible to estimate the effective aspect ratio of evenly distributed filler particles that act as diffusion retardants for any polymer-filler combination. In our case, the OTR decrease by 6 % compared to pristine samples for the 2 wt.% and by 17 % for the 10 wt.% nanoclay-PA composite indicates that the direct effect of the filler particles is modest. By plotting the change in OTR against the weight percentage of the filler in polymer we were able to estimate that the approximate average filler particle aspect ratio is ~5.9 (Fig. 7). It must be noted that this is an estimation for an ideal case of defect-free polymer with homogeneously dispersed particles, aligned perfectly perpendicular to the gas diffusion direction. To overcome this masking effect of imperfections and orientation bias, we can assume that the actual aspect ratio is much bigger. Indeed, from the SEM image of the agglomerates (see Fig. 2) one can estimate that for a single platelet, the aspect ratio is easily more than excess of 100. By considering the latter we can assume that the calculated aspect ratio therefore represents merely the apparent aspect ratio composing of the average projection of the particles' geometry onto a plane perpendicular to the diffusion direction (see Fig. 8). In other words, every randomly

oriented nanoclay platelet seems to have an aspect ratio that is the ratio of its perpendicular and parallel projections in respect to the diffusion direction. By doing appropriate substitution into Eq. 1, we can rewrite it by using the orientation angle φ of the nanoclay particles:

$$\frac{P_f}{P_u} = \frac{\Phi_P}{1 + \left(\frac{1}{2 \tan \varphi}\right) \Phi_F} \quad (2)$$

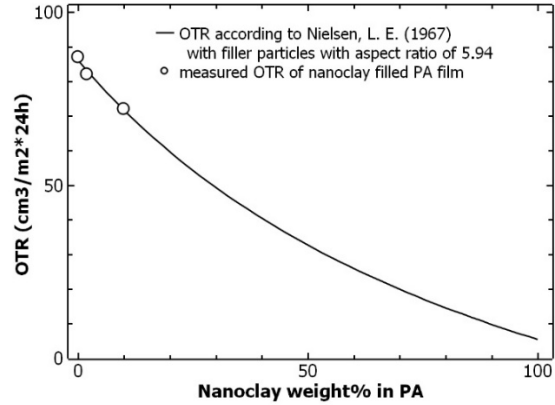


Fig. 7. Approximated OTR vs. loading of planar additives with aspect ratio 5.94 (line) according to Nielsen L. E. [18] and experimental OTR values of the prepared PA films with different nanoclay loading (circles)

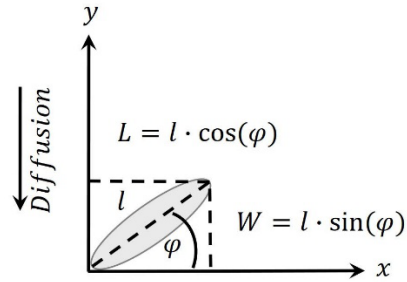


Fig. 8. A thin nanoclay particle (high aspect ratio) orientation at an angle taken as an approximation for pseudo-particle with respective side dimensions W and L

Thus, the obtained apparent aspect ratio of 5.9 corresponds to the average angle of 9.5° between the particle's axis and the film surface plane which is at 90° angle with the diffusion normal direction. Considering this, we can now estimate the maximum limiting angle that the particles' orientation can have with respect to the film surface to derive the desired OTR performance at a given loading. E.g., from Fig. 9 we can see that in order to achieve the desired OTR value of 10 cm³/m²·24 h at 10 wt.% loading of nanoclay in polyamide, the maximum average angle that the platelets can have is ~0.4°. This is a rather small angle. Apparently, ensuring an average deviation of equal to or less than this value for all the platelets in a bulk is difficult for the films made by the hot-pressing technique. Increasing the loading to 50 wt.% would allow for a more realistic tolerance of ~4° (see Fig. 9), but such a high loading would probably make the film unusable due to the significant replacement of the polymer. Increasing the loading beyond 10 wt.% is problematic not only because of the potential price increase of the film due to the higher price of nanoclay when compared to PE, but also because of its other physical properties.

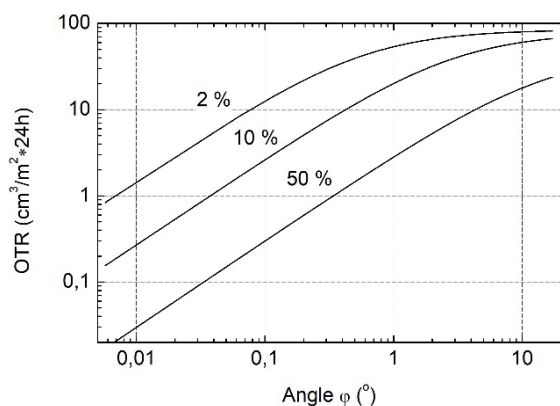


Fig. 9. OTR dependence on the angle of the filler (nanoclay) particles at different filler weight percentages

At 10 wt.% the yield strength of the polymer film with nanoclay additive is increased by ~21 % as compared to the pristine PA film: 38.4 MPa for pure PA and 46.5 MPa for the nanoclay-PA composite (Fig. 10). This indicates that there is good bonding between the nanoclay particles and the polymer. Yield strength is more important than stress at a break in most packaging applications, so the mechanical properties have improved for most barrier film uses.

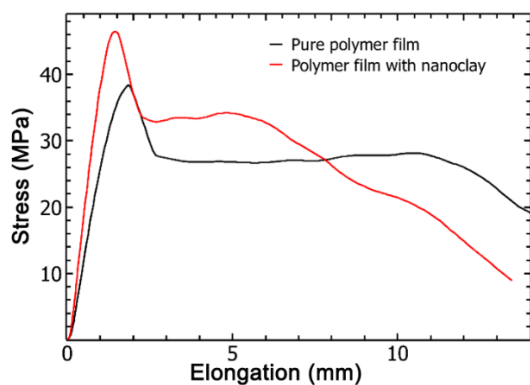


Fig. 10. Comparison of tensile strength of pure PA polymer film and with 10 % nanoclay additive

This is in good accordance with previous works on polymer/additive composites, which suggest that the mechanical properties of a composite are determined by the interfacial strength and the surface contact area of the filler [19, 20]. The film showed a somewhat decreased necking region where there is an extension at a constant force (Fig. 10). The apparent shortening of the constant force region could be attributed to the relatively lower amount of polymer chains, which are replaced by nanoclay particles. The stress-strain behavior of the films at higher than 10 wt.% loading was not tested, but most obviously the increase in rigidity would be more pronounced. High concentrations of nanoclay lead to coloration, as was shown by Kim and Sang-Ho who studied EVOH copolymer nanocomposites and found that the polymer film developed an increased absorption preferably in the blue region as the concentration of nanoclay was increased up to 7 wt.% [3]. We made a similar observation qualitatively – the prepared 10 wt.% nanoclay-polymer mix appeared reddish brown before hot pressing.

Due to the latter considerations, the amount of filler nanoclay should be kept as low as possible and at the same time high enough to ensure the minimum desired OTR performance. As shown, one way to comply with this requirement would be to use 10 wt.% of nanoclay content and orient the particles at an angle of 0–0.4 degrees in respect of the film surface. However, while the melt state mixing technique by twin-screw extrusion provides good exfoliation of nanoclay in PA, the simple hot-pressing technique does not provide control of the orientation of the particles to achieve satisfactory OTR performance, hence the final orientation of the particles should be done via alternative methods. One possible technique that could yield better control of the orientation of the particles is actually the industrially used blown film technique for film formation. During this process, the final stretching of the film is done by expanding it in melt state by using air pressure. It is also known to impose greater forces on the agglomerates in order to separate single nanoclay platelets and orientate the polymer molecules as well as the clay platelets to a greater extent [21].

4. CONCLUSIONS

Present work shows that the addition of nanoclay to hot-pressed industrial-grade polyamide films up to the content of 10 wt.% can improve the films' oxygen barrier properties without degrading their physical or visual properties. However, the obtained oxygen barrier performance is rather modest. At 10 wt.% of nanoclay loading, the oxygen transmission rate of the film decreased by ~17 % as compared to this of the pristine polymer film. At the simplest approximation by using the Nielsen equation, this corresponds to a film containing dispersed platelet shaped particles oriented in plane with this of the film surface and having an average aspect ratio of 5.9. This is considerably lower than that of a single nanoclay platelet, which has an aspect ratio of >100. XRD analyses indicated a nearly complete exfoliation of the nanoclay particles, hence we propose that the modest oxygen barrier performance of the composite film was not caused by insufficient exfoliation but is rather an indication of an imperfect orientation of the dispersed nanoclay platelets relative to this of the oxygen diffusion direction. Considering this notion, for the prepared film containing 10 wt.% of nanoclay, we get that on average the particles are oriented at 9.5 degrees relative to the polymer film surface.

Latter findings suggest that the direct melt-mixing technology by twin-screw extrusion shows great promise for industrial use of polyamide with nanoclay additives as it enables effective break-down of larger nanoclay agglomerates and good filler particle dispersion in the polymer. The addition of up to 10 wt.% of PA increases the tensile strength of the films while not causing noticeable coloration. Nevertheless, the industrially relevant OTR performance of 10 cm³/m²·24 h is not easily obtainable with a simple process of hot pressing the film to the required micrometre-scale thickness. By our estimates, it requires a rather tight ~0.4° maximum tolerance for the orientation of exfoliated nanoclay platelets. We propose that the bubble extrusion technique could offer better control of the orientation of the nanoclay particles along the film's surface

plane. Further systematic testing and refining of the mixing and film-making methods shall be carried out in the future to elaborate efficient means for producing cost-effective low OTR food packaging materials.

Acknowledgments

The authors of the project would like to thank Estonian Science Agency's grants IUT34-27, PRG1198, the European Regional Development Fund project TK134 "Emerging orders in quantum and nanomaterials" for funding and Estiko Plastar AS, a private enterprise, for providing access to the OTR and tensile measurement apparatus. This work was supported by Estonian Research Council grant PRG1198.

REFERENCES

- Vanderzant, C., Hanna, M.O., Ehlers, J.G., Savell, J.W., Smith, G.C., Griffin, D.B., Terrell, R.N., Lind, K.D., Galloway, D.E. Centralized Packaging of Beef Loin Steaks with Different Oxygen-Barrier Films: Microbiological Characteristics *Journal of Food Science* 47 1982: pp. 1073–1079. <https://doi.org/10.1111/j.1365-2621.1982.tb07622.x>
- Kim, S.W., Cha, S.H. Thermal, Mechanical, and Gas Barrier Properties of Ethylene-Vinyl Alcohol Copolymer-Based Nanocomposites for Food Packaging Films: Effects of Nanoclay Loading *Journal of Applied Polymer Science* 131 (11) 2014: pp. 40289. <https://doi.org/10.1002/app.40289>
- Stiller, B. The Effect of Montmorillonite Nanoclay on Mechanical and Barrier Properties of Mung Bean Starch Films 2008 All Theses. 504. https://tigerprints.clemson.edu/all_theses/504
- Cerisuelo, J.P., José, A., Aucejo, S., Gavara, R., Hernández-Muñoz, P. Modifications Induced by the Addition of a Nanoclay in the Functional and Active Properties of an EVOH Film Containing Carvacrol for Food Packaging *Journal of Membrane Science* 423–424 2012: pp. 247–256. <https://doi.org/10.1016/j.memsci.2012.08.021>
- García, A., Eceolaza, S., Iriarte, M., Uriarte, C., Etxeberria, A. Barrier character improvement of an amorphous polyamide (Trogamid) by the addition of a nanoclay *Journal of Membrane Science* 301(1–2) 2007: pp. 190–199. <https://doi.org/10.1016/j.memsci.2007.06.018>
- Thakur, A.K., Kumar, P., Srinivas, J. Studies on Effective Elastic Properties of CNT/Nano-Clay Reinforced Polymer Hybrid Composite *IOP Conference Series: Materials Science and Engineering* 115 2016: pp. 012007. <https://doi.org/10.1088/1757-899X/115/1/012007>
- Hussain, F., Dean, D., Haque, A. Structures and Characterization of Organoclay-Epoxy-Vinylester Nanocomposites *Proceedings of IMECE 2002 ASME International Mechanical Engineering Congress & Exposition* 2002: pp. 1–8. <https://doi.org/10.1115/IMECE2002-33552>
- Choudhary, S., Sengwa, R.J. Intercalated Clay Structures and Amorphous Behavior of Solution Cast and Melt Pressed Poly(ethylene oxide)–Clay Nanocomposites *Journal of Applied Polymer Science* 2014: pp. 1–9. <https://doi.org/10.1002/app.39898>
- Yasmin, A., Abot, J.L., Daniel, I.M. Processing of Clay/Epoxy Nanocomposites with A Three-Roll Mill Machine *MRS Online Proceedings Library* 740 (37) 2003: pp. 75–80. <https://doi.org/10.1557/PROC-740-13.7>
- Kusmono, Z., Ishak, A.M. Effect of Clay Addition on Mechanical Properties of Unsaturated Polyester/Glass Fiber Composites *International Journal of Polymer Science* Article ID 797109 2013. <https://doi.org/10.1155/2013/797109>
- Yap, Y.P., Chow, W.S. Effect of Mixing Sequences on the Flexural and Morphological Properties of Epoxy/Organo-Montmorillonite Nanocomposites *Journal of Composite Materials* 43 (20) 2009: pp. 2269–2284. <https://doi.org/10.1177/0021998309344936>
- Lincoln, D.M., Vaia, R.A., Wang, Z.G., Hsiao, B.S. Secondary Structure and Elevated Temperature Crystallite Morphology of Nylon-6/layered Silicate Nanocomposites *Polymer* 42 (4) 2001: pp. 1621–1631. [https://doi.org/10.1016/S0032-3861\(00\)00414-6](https://doi.org/10.1016/S0032-3861(00)00414-6)
- Krishnan, P.S.G., Wisanto, A.E., Osiyemi, S., Ling, C. Synthesis and Properties of BCDA-based Polyimide–clay Nanocomposites *Polymer International* 56 (6) 2007: pp. 787–795. <http://dx.doi.org/10.1002/pi.2209>
- Faghihi, K., Abootalebi, A.S., Shabanian, M. New clay-Reinforced Polyamide Nanocomposite Based on 4-Phenylenediacrylic Acid: Synthesis and Properties *Journal of Saudi Chemical Society* 17 (2) 2013: pp.191–197. <http://dx.doi.org/10.1016/j.jscs.2011.03.007>
- Abdelwaha, M., Codou, A., Anstey, A., Mohanty, A.K., Misra, M. Studies on the Dimensional Stability and Mechanical Properties of Nanobiocomposites from Polyamide 6-filled with Biocarbon and Nanoclay Hybrid Systems *Composites Part A* 129 2020: pp. 105695. <https://doi.org/10.1016/j.compositesa.2019.105695>
- Battagazzore, D., Sattin, A., Maspoch, M.L., Frache, A. Mechanical and Barrier Properties Enhancement in Film Extruded Bio-Polyamides with Modified Nanoclay *Polymer Composites* 2018: pp. 1–12. <https://doi.org/10.1002/pc.25056>
- Nielsen, L.E. Models for the Permeability of Filled Polymer Systems *Journal of Macromolecular Science Part A: Chemistry* 5 1967: pp. 929–942. <https://doi.org/10.1080/10601326708053745>
- Eirasa, D., Pessan, L.A. Mechanical Properties of Polypropylene/Calcium Carbonate Nanocomposites *Materials Research* 12 (4) 2009: pp. 517–522. <https://doi.org/10.1016/j.matlet.2005.10.020>
- Zhang, X., Loo, L.S. Morphology and Mechanical Properties of a Novel Amorphous Polyamide/ Nanoclay Nanocomposite *Journal of Polymer Science: Part B: Polymer Physics* 46 (23) 2008: pp. 2605–2617. <https://doi.org/10.1002/polb.21585>
- Ward, D., Teh, J., Ho, K., Marler, J., Aube, N. Oxygen Permeability Enhancements in Octene LLDPE Film Affected by LDPE Blending and Crystalline Orientation Changes *Nova Chemicals Corporation* 2007.



© Paara et al. 2022 Open Access This article is distributed under the terms of the Creative Commons Attribution 4.0 International License (<http://creativecommons.org/licenses/by/4.0/>), which permits unrestricted use, distribution, and reproduction in any medium, provided you give appropriate credit to the original author(s) and the source, provide a link to the Creative Commons license, and indicate if changes were made